Journal of Coastal Research	11	4	1180–1194	Fort Lauderdale, Florida	Fall 1995

On the Formation of Bars by the Action of Waves on an Erodible Bed: A Laboratory Study

Vincent Rey†, Alan G. Davies‡ and Max Belzons†

†Département de Physique des Systèmes Désordonnés SETT, URA 1168 du CNRS
Université de Provence Centre de Saint-Jérôme Case 161
13397 Marseille Cedex 13, France

‡School of Ocean Sciences
University of Wales
Marine Science Laboratories
Menai Bridge
Anglesey, Gwynedd LL59 5EY
United Kingdom

ABSTRACT

REY, V.; DAVIES, A.G. and BELZONS, M., 1995. On the formation of bars by the action of waves on an erodible bed: a laboratory study. *Journal of Coastal Research*, 11(4), 1180–1194. Fort Lauderdale (Florida). ISSN 0749-0208.

Sand bars having spacing equal to half the surface wavelength may be formed by the action of partially-standing waves on an erodible bed. Here the stages of development of a patch of bars has been investigated in a wave tank, using rapid, accurate, ultra-sonic detection systems to monitor both the changing bed profile and the evolving surface wavefield. Initially, small-scale ripples formed on a (flattened) bed surface. These ripples varied in size according to position in the wave envelope, and had asymmetrical profiles due to asymmetry in the near-bed oscillatory motion. Vortex shedding from the ripples gave rise to regions of net sediment accumulation (bar crests) and erosion (troughs) linked to position in the wave envelope. The bars formed with wavelength satisfying the Bragg condition and with bar crests positioned down-wave of the antinodes of elevation. As expected, this produced an increase in the overall reflection coefficient of the bar patch as the bars grew in height. The presence of the small-scale ripples had only a minor effect on the reflection coefficient, the flow being essentially inviscid away from the boundaries of the motion and the ripple wavelength being far smaller than the surface wavelength. However, the ripples played an important role in dissipating wave energy in the tank, wave dissipation factors being 3 or 4 times larger than equivalent values for laminar flow above a smooth bed. The present observations of the resonant interaction between surface waves and an erodible bed are believed to be the most detailed and accurate to have been reported to date.

ADDITIONAL INDEX WORDS: *Wave tank, resonant interaction, sand bed erosion, wavefield, ultra-sonic detection.*

INTRODUCTION

The formation of sand bars off beaches by wave action has been the subject of a number of investigations in both the field (*e.g.* SAYLOR and HANDS, 1970; SHORT, 1975a; DETTE, 1980) and the laboratory (*e.g.* SCOTT, 1954; BROOKE-BENJAMIN *et al.*, 1987; O'HARE and DAVIES, 1990). In the field, bar patches have been reported comprising up to 20 shore-parallel ridges, with crest to trough heights of the order of 1 m, and with spacings in the range of ten metres to several hundred metres (increasing offshore with increasing depth). A variety of possible explanations for the formation of such bars has been proposed, some of which relate to the behaviour of long-period infragravity waves off beaches (discussed by O'HARE and DAVIES, 1990). The simplest explanation, which may be applicable when a partially-standing wavefield is caused by reflection from a beach, is that regions of sediment accumulation and erosion arise in relation to the nodes and antinodes of surface elevation as a result of spatial non-uniformities in the net transport of sediment (CARTER *et al.*, 1972; SHORT, 1975b; BOWEN, 1980). Bars formed in this way are expected to have spacing equal to approximately half the surface wavelength (O'HARE and DAVIES, 1990). Moreover, the growth of such bars will give rise to slow changes in the partially-standing wavefield, which may enhance or inhibit the further development of the bars, depending upon the nature of the dominant (small-scale) sediment transport processes.

The possibility of a resonant interaction between surface waves and the bed was discussed by DAVIES (1982), and DAVIES and HEATHERSHAW (1984), on the basis of theoretical analysis and laboratory experiments with fixed sinusoidal bars. It was shown that, if progressive waves are nor-

92117 received 15 October 1994; accepted in revision 2 October 1994.

mally incident on a patch of bars having spacing equal to half the surface wavelength, strong (BRAGG) reflection of the incident waves may occur for even a small number of bars of modest amplitude. More recently, BRAGG resonances have also been demonstrated experimentally and theoretically in the case of a fixed bed having a profile consisting of the superimposition of two sinusoids, hence giving rise to subharmonic effects (BELZONS *et al.*, 1991; GUAZZELLI *et al.*, 1992). DAVIES and HEATHERSHAW (1984) suggested that, on an erodible bed, the partially-standing wavefield both over and up-wave of a bar patch might serve to reinforce the existing bars and lead to the development of new bars up-wave of the original patch. This 'coupling' between the waves and the bed would lead to increased reflection and, hence, further bar growth and so on until a final limiting bed profile was attained. In this way it was argued, a beach might protect itself from the full impact of wave attack. HEATHERSHAW and DAVIES (1985) described some observations of the movement of a thin veneer of sand on a fixed bar patch, which suggested that this hypothesis might be valid. However, insufficient sand was present to study the phenomenon of bar growth fully.

The formation of bars beneath purely standing waves above a fully erodible bed was demonstrated in the laboratory by NIELSEN (1979). Beneath standing waves, bottom friction gives rise to a mass transport velocity field comprising closed, quarter-wavelength cells; the direction of the residual velocity at the edge of the (thin) bottom boundary layer is from nodal to antinodal position (LONGUET-HIGGINS, 1953; JOHNS, 1970). NIELSEN'S experiment was conducted with a fine sand for which the dominant transport mechanism was a suspended load. In particular, sediment grains supended by the underlying oscillatory wave action were given a net transport in the direction of the residual motion, such that bar crests formed beneath the antinodes of elevation and troughs formed beneath the nodes.

In the more complicated case of a partially-standing wavefield, the near-bed mass-transport velocity comprises the above cellular pattern together with a residual component in the direction of wave advance associated with the progressive wave. Thus the near-bed mass transport velocity has a forward component which is modulated in strength depending upon position in the partially-standing wave envelope. CARTER *et al.* (1972) argued that bars would form in this case only if a reversal occurred in the direction of the near-bed mass transport velocity at some position in the wave envelope. In particular, they showed that if the reflection coefficient R, defined as the ratio of the reflected to incident wave amplitude, is greater than 0.414, then such a reversal occurs at the point midway between each antinode and the next (down-wave) node. In practice, however, a reversal of the mass transport velocity is not a necessary condition for bar formation, as shown by SCOTT (1954) and O'HARE and DAVIES (1990) in whose experiments the reflection coefficient was typically lower than 0.414. O'HARE and DAVIES concluded that a modulation in the mass transport velocity and, hence, in the sediment transport rate is sufficient to initiate bar formation.

More generally, O'HARE and DAVIES found that the interaction between the surface wavefield and the bed depends critically upon the position of the growing bar crests in relation to the partially-standing wave envelope. If the dorminant sediment transport process is suspended load, then bars form with crests beneath the antinodes of elevation, as in Nielsen's experiment with fine sediment. However if near-bed sediment transport, specifically net transport associated with vortex shedding from small-scale ripples, is dominant, then bars form with crests between antinodes and the next down-wave node. The positioning of the crests was found by O'HARE and DAVIES to be very significant in terms of the ability of bars to reflect incident wave energy. In the former case (*i.e.*, suspended load dominant), the growth of bars was accompanied by little increase in the reflection coefficient on the up-wave side of the bar patch. By comparison, in the latter case (*i.e.*, 'bedload' dominant), the reflection coefficient increased steadily as the bars grew, and sometimes quite dramatically so, leading to wave breaking and the destruction of the bar patch. The evolution of sand bars and of the associated (monochromatic) wave field has been modelled by O'HARE (1992), whose results have explained the importance of the positioning of the bar crests in the sense discussed above and, more generally, have confirmed the validity of the hypothesis of DAVIES (1982) concerning resonant surface-wave/bed interaction and the growth of bars.

Although O'HARE and DAVIES (1990) were able to make rapid and accurate measurements of the surface waves up-wave and down-wave of an evolving bar patch in a wave tank, using parallel-wire gauges, their capabilities were limited where

detailed observation of the time-varying bed profile was concerned. In the present paper, similar experiments on the growth and stability of sand bars are reported in which this limitation has been overcome by use of an acoustic transducer, mounted on a computer-controlled carriage (see REY, 1991), to monitor the changing bed elevation. This set-up was capable of digitizing the bed profile, rapidly and accurately, in respect to both small-scale ripples which formed on the short timescale of a few minutes and also larger-scale bars which evolved more slowly on the timescale of tens of minutes. The surface wave field was also monitored accurately using a second acoustic device (though the procedure for interrogating the wavefield over the evolving bed was only really suitable for the measurement of changes on the longer timescale of bar formation). The aim of the experiments was to use this accurate, well controlled measuring system to monitor the simultaneous evolution of the wavefield and the bed profile, starting with the (rapid) formation of small-scale ripples on an initially flattened erodible bed and continuing through to the (slower) formation of bars by resonant surface-wave/bed interaction. The results, which are analyzed in respect to the ripples and bars separately, are consistent with those of O'HARE and DAVIES (1990) for the case of sediment transport dominated by near-bed processes. In other words, the bars in the present experiments were reflective to a significant degree.

In Section 2, the experimental set-up is described and, in Sections 3 and 4, the results are presented and discussed. In Section 3, a Fourier analysis of the evolving bed is carried out in order to separate the small-scale ripples from the bars and investigate the relationship between the measured ripple heights and wavelengths and the near-bed oscillatory flow. In addition, a harmonic analysis of the wavefield is performed both over the bar patch and on its up-wave side and some estimates are made of the wave energy dissipation factor. It is believed that the present laboratory experiments represent the most accurate set of observations of an evolving bar field which have been reported to date.

EXPERIMENTAL TECHNIQUES

The experiments were carried out in a glass-walled wave tank 4.7 m long and 0.39 m wide (see Figure 1). At one end of the tank a paddle wave maker, powered by a stepping motor, produced gravity waves in water of mean depth 6 cm. The stepping motor was monitored by a micro computer which enabled the fundamental frequency of the wave to be defined very accurately. The amplitude of the paddle was controlled by the stroke of the eccentric. For fixed frequency, water depth and immersion depth of the paddle, the amplitude of the surface wave and its harmonic content were controlled by the amplitude of the paddle and were thus easy to reproduce. In the experiments presented hereafter, the fundamental frequency f_0 was set at 1.5 Hz with an accuracy of order 0.0001 Hz. The wave maker amplitude was either A_{wm} = 8 mm or 14 mm, corresponding respectively to an incident wave amplitude of 4.6 or 7.7 mm. Reflection of these waves by a sloping beach at the other end of the wave tank produced a field of partially standing waves. In water of constant depth 6 cm and with f_0 = 1.5 Hz, the reflection coefficient of the beach was about R_B = 0.21 for A_{wm} = 8 mm, and R_B = 0.15 for A_{wm} = 14 mm. More generally for low waves, the reflection coefficient was a rapidly decreasing function of the wave frequency, being practically zero at 3 Hz and above. As a result, for nonlinear waves of given height at the fixed fundamental frequency (1.5 Hz), R_B diminished as the harmonic content of the wavefield increased.

In order to examine the response of an erodible bed to this partially-standing wave field, a layer of artifical sand was placed over the glass bottom of the wave tank in a region extending from 1 m down-wave of the wave maker to 1 m up-wave of the beach. This artificial sand consisted of glass spheres manufactured by the Ballotini company, with density $\rho_s = 2{,}700\ kg \cdot m^{-3}$, a median diameter D of 0.080 mm and with 79% of the spheres having diameter in the range 0.055 mm to 0.105 mm (dispersion 0.025 mm). Prior to each experiment, the sand layer was carefully leveled to a mean thickness of 12.5 mm with an accuracy of about 1 mm.

The detection of the bed profile was achieved very accurately using a high frequency ultra sonic sensor (Model WS25-5, manufactured by Ultran Laboratories Inc.). In this sensor, the transducer is a piezo-electric quartz with a resonating frequency of 5 MHz, which is used both for transmitting and receiving. This quartz is mounted adjacent to an acoustic lens which focuses the impulse signal on to the reflector. The signal is then echoed and received after a time lag ΔT proportional to the distance between sensor and reflector. This process is repeated at a frequency of

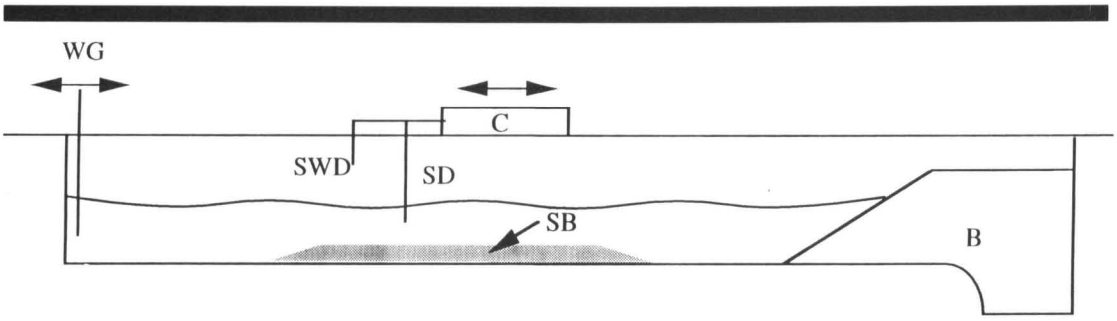

Figure 1. Sketch of the wave tank showing the wave maker (WM), the beach (B), the carriage (C), the sand detector (SD), the surface wave detector (SWD) and the sand bed region (SB).

200 Hz. In the present experiments, the acoustic lens was placed just under the water surface in order to avoid unwanted echoing from the surface, and the focal length was chosen so as to focus the impulse in the vicinity of the bed. The system was mounted on a carriage which could be translated along the tank by a stepping motor controlled by a microcomputer. The emission and reception of the signal, the time lag ΔT, and the position of the sensor along the centre line of the tank were monitored by the computer. This set-up could digitize the entire bed profile in a very short time interval (about 60 sec) with an accuracy of ± 0.2 mm in height and ± 0.05 mm in the abcissa. The data were stored in the computer for subsequent processing.

The second sensor which was used for the detection of the surface waves was an ultra sonic ranging module (Model E-201, manufactured by Masa Products Corporation). This sensor comprises two quartz transducers, one for emitting and one for receiving, operating at the frequency of 0.215 MHz with a maximum repetition rate of 100 pulses/sec. These transducers which are highly directional were mounted on a plate fixed to the carriage, the one transducer being slightly inclined in respect of the other in order to maximize the reflection of the acoustic pulse from the water surface. The monitoring of this second system was also performed by the computer. For a fixed abcissa (*i.e.*, fixed position along the tank), 40 records of surface elevation were taken at regular intervals during each wave period. From these records, the surface wave envelope and the harmonic content of the waves were subsequently obtained. Since between 200 and 220 recording positions were needed to monitor the wave field adequately, the total time needed for recording was about 20 min. Although this was greater than the time scale for ripple growth (about 15 min), the system was suitable for monitoring the response of the wave field to slowly-evolving sand bars. Calibration of the system revealed an accuracy of order ± 0.1 mm in the wave amplitude and of order ± 0.05 mm in the abcissa.

EXPERIMENTAL RESULTS

The experiments were conducted with a wave frequency $f_0 = 1.5$ Hz above a sand bed of mean thickness 1.25 cm, and total length L = 160 cm, the water depth on either side of the region of erodible bed being h = 6 cm. The results presented relate to a typical experiment of a 7 hour duration, though some comments are made relating to other experiments which are not discussed in detail.

The sequence of observations described below reveals, firstly, the formation of small-scale ripples and, secondly, the development of a regular patch of sand bars on a larger scale. The very precise acoustic method used for the detection of the bed allowed the simultaneous measurement of these different bedform types, as depicted in the typical sequence in Figures 2 to 6. The associated surface wave records, up-wave and over the sand bed, were analyzed in terms of the harmonic composition of the wave field as described below. The nominal wave amplitude was 7.7 mm except on two occasions, at the start of the experiment and after 180 min when the wave amplitude was temporarily decreased to 4.6 mm. These lower waves did not disturb the sediment and so produced no modification to the bed shape which was generated entirely by the larger waves.

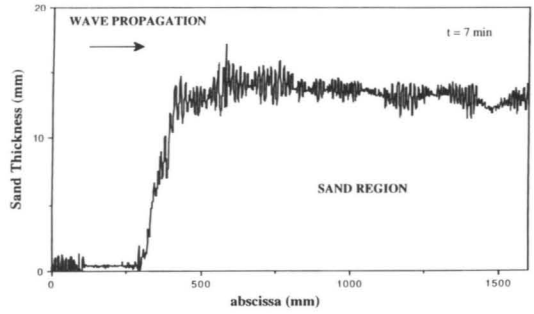

Figure 2. Bed profile after 7 min of wave action showing the early formation of ripples. The largest ripples were in regions which later became troughs, and the smallest ripples in regions which later became crests.

Analysis of the Ripples and Sand Bars

The raw data in Figures 2 to 6 shows the profile of bed elevation along the centre-line of the tank at different stages in the experiment, the sand patch occupying the region from about 300 mm to 1,600 mm on the abscissa. After 7 min (Figure 2), there was clear evidence of small-scale ripple formation. The wavelengths and heights of these ripples were modulated according to their position in the partially-standing wave field; in particular, the largest ripples developed beneath the nodes of elevation (*i.e.*, where the horizontal velocity amplitude was greatest), and the smallest ripples beneath the antinodes. Later in the experiment, these regions of large and small ripples became the positions of bar troughs and crests respectively. An initial indication of bar formation was obtained after 12 min (Figure 3) and, even at this early stage, the modulation in the

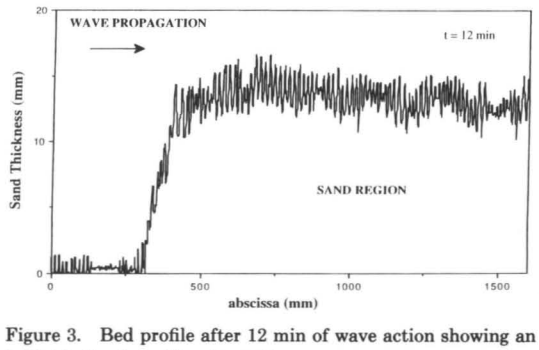

Figure 3. Bed profile after 12 min of wave action showing an initial indication of bar formation.

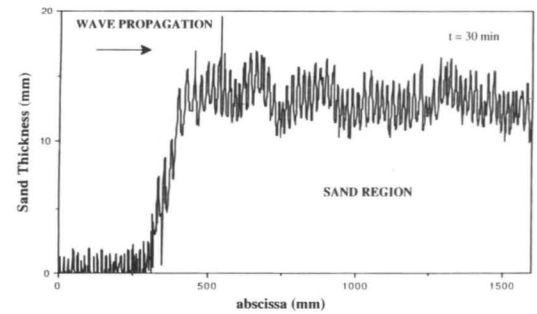

Figure 4. Bed profile after 30 min of wave action.

wavelengths and heights of the ripples was less distinct. After 30 min (Figure 4), the development of the bars was well advanced, and the ripple sizes appeared fairly uniform. After 60 min (Figure 5), the positions of six bar crests were well established, the mean wavelength of the bars being about 21 cm. This is in accordance with the Bragg condition, the measured wavelength over the erodible bed being 42 cm, and the wavelength calculated using the dispersion relation with a water depth of 4.75 cm being 42.2 cm. From this point onward, ripple size started to increase in the region of the bar crests and to decrease in the troughs, a trend which was evident initially in Figure 5 and which was confirmed by subsequent profiles including the final profile after 420 min (Figure 6). It may be noted in Figure 6 that, as a result of a net movement of sand in the up-wave direction, an additional (low) bar developed slowly during the experiment with its crest at about 200 mm on the abscissa. Sediment transport was dominated by the effects of vortex shedding from small-scale ripples, with net up-wave transport resulting from asymmetry in the ripple profiles (this, in turn, being associated with asymmetry in the strengths of the vortices shed in successive half cycles). In relation to O'HARE'S (1992) model, the experiment was therefore of the 'bedload' dominated type.

The small-scale ripples have been distinguished from the bars by using a Fast Fourier Transformation (FFT) of the bed profile. This is presented in Figure 7 for the bed profile after 30 min of wave action (*i.e.* the profile in Figure 4). The portion of the bed analyzed corresponds to the first 1,024 points of the bed-level file (a distance of 780 mm on the abscissa) following the general change in level at the start of the sand patch. The part of

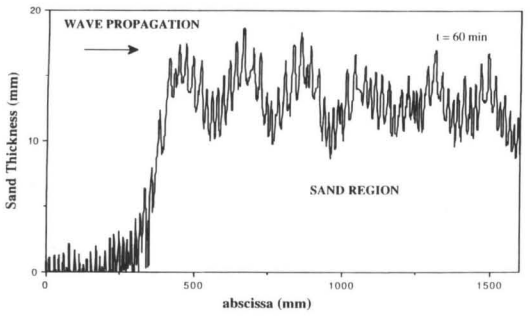

Figure 5. Bed profile after 60 min of wave action.

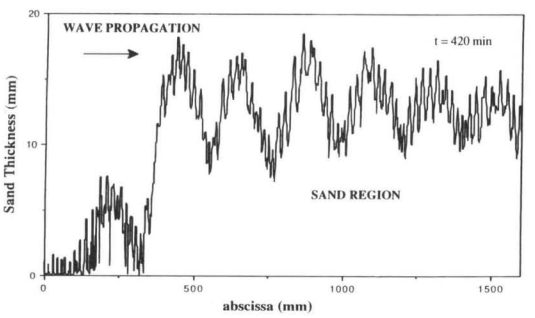

Figure 6. Final bed profile after 420 min of wave action.

the spectrum below the wavenumber giving the first significant minimum may be identified with the bars, while the part extending from this wave number to that of the second significant minimum may be identified with the ripples. These wave numbers are marked with arrows on Figure 7. The profiles of the bars (Figure 8) and of the ripples (Figure 9) have been obtained from the inverse FFT of the appropriately filtered spectrum in the respective cases. The bars were only partly developed after 30 min of the experiment, particularly at the up-wave end of the sand patch. The ripples were fairly uniform in height and wavelength throughout the patch at this time.

For the typical sequence in Figures 2 to 6, the threshold for ripple formation on the flattened bed was observed at A_{wm} = 12 mm, that is for a surface wave amplitude of 6.6 mm. Using linear theory, this corresponds to a near bed orbital velocity amplitude of U_0 = 8.2 cm/sec, and hence a mobility number $M = U_0^2/\gamma gD$ of about 5 where the relative density $\gamma = (\rho_s - \rho_f)/\rho_f$, ρ_f = fluid density, g is the acceleration due to gravity, and D is the median grain diameter. With A_{wm} = 14 mm, ripple formation occurred after a few minutes beneath the nodes of the partially standing waves. As noted earlier, the wavelengths (λ) and heights (η) of the ripples were initially greatest beneath the nodes. The mean values of λ and η, which were relatively small initially, increased with time to fairly constant values after about 60 min (Figure 10). The values of λ and η were fairly well correlated throughout the experiment, with a linear correlation factor reaching a value of order 0.8 after about 30 min. The associated ripple steepness η/λ remained approximately constant with a value of 0.18. However after a run time of about 60 min, there was a tendency for the largest ripples to occur on the bar crests, *i.e.*, beneath the antinodes of the partially standing wave; this was so up to the end of the experiment after 7 hours. It may be noted in Figure 10, where the results from a second run are labelled with circled symbols that for given initial conditions the mean values of λ and η at a fixed time in the experiment are fairly well reproduced. For all the runs carried out, the ripples were initially long-crested. However after about 10 min, they became somewhat three-dimensional, though still with generally long crests.

Analysis of the Surface Waves

When the sand bed was flat, the standing wave component in the wave field was due entirely to back-reflection from the beach. (The reflection coefficient calculated by the method of REY (1992) for a long bar with the initial geometry of the sand bed was found to be very small (about 0.015).) From the wave envelope measured along the tank, the up-wave (R_{uw}) and down-wave (R_{dw}) reflection coefficients for the fundamental frequency were obtained. Further calculations were made relating to the wavefield at the start of the experiment and also after 180 mn, with nominal incident amplitudes of 4.6 mm and 7.7 mm in each case, corresponding to conditions below and above the threshold of ripple formation, respectively. This exercise was carried out to check that the presence of suspended sediment had no significant effect on the wave field. There was little further change in either the wavefield or the bed profile after 180 min.

The wave amplitude for the fundamental and first two harmonics of the wave field are displayed

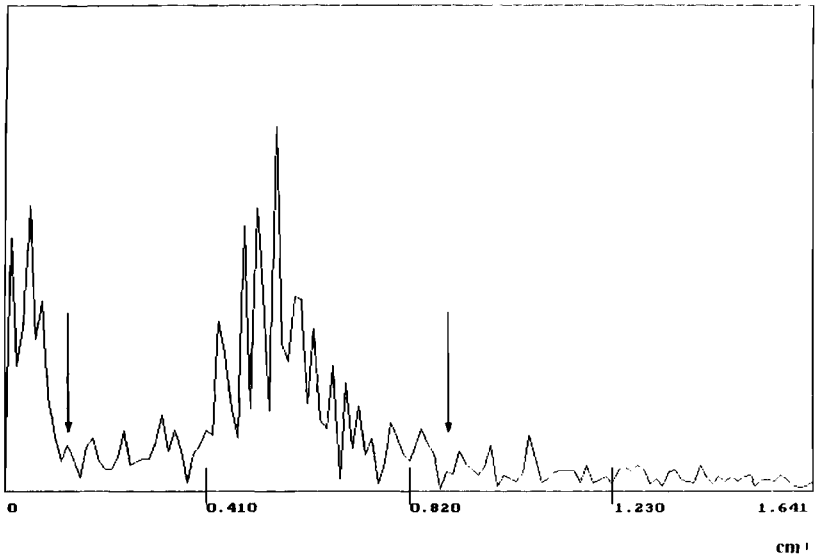

Figure 7. Fourier spectrum of a part of the bed profile of Figure 4 extending from abscissa 457 to 1,237 mm. The part of the spectrum to the left of the first arrow may be attributed to bars, whereas the part between the arrows may be attributed to ripples. On the abscissa the wavenumbers are in cm^{-1}; the ordinate represents bed amplitude on an arbitrary scale.

together with the bed profile in Figures 11a to d. Figures 11a and b correspond to the start of the experiment (time 0 min) with A_w = 4.6 mm and A_w = 7.7 mm respectively, whereas Figures 11c and d correspond to time 180 min, also with A_w = 4.6 mm and A_w = 7.7 mm respectively. With A_w = 7.7 mm a suspended sediment load due to vortex shedding from the rippled bed was present while the measurements of the wave envelope were made. The results for R_{uw} and R_{dw} for which the accuracy is about ±0.02, were as follows: Table 1: The data indicate that the down-wave reflection coefficient was independent of the evolution of the sand bed, and due to the differing amounts of beach reflection associated with the different incident wave amplitudes. By comparison, on the up-wave side of the sand patch, an increasing reflection coefficient was measured as the bars developed. This increase was of approximately the same magnitude for the two values of wave amplitude examined, *i.e.* from 0.15 to 0.27 for A_w = 4.6 mm, and from 0.10 to 0.23 for A_w = 7.7 mm. This increase is associated with the Bragg reflection condition which was well satisfied, as can be seen in Figure 11c.

Table 1. *Reflection coefficients versus wave amplitudes.*

R_{uw}	A_2 = 4.6 mm	A_w = 7.7 mm	R_{dw}	A_w = 4.6 mm	A_2 = 7.7 mm
0 min	0.15	0.10	0 min	0.205	0.16
180 min	0.27	0.23	180 min	0.21	0.15

Some further observations may be made about the wave field, particularly following the formation of the sand bars (Figures 11c and d). Firstly, the oscillation in the wave amplitude at the fundamental frequency diminished across the bar patch, as expected for waves having frequency centred in the first Bragg forbidden band. However, the transmission coefficient on the down-wave side was rather lower than that which would have occurred in the absence of energy losses; for example, associated with the reflection coefficient of 0.27 on the up-wave side in Figure 11c, a transmission coefficient of 0.96 might have been expected. In practice, a general decrease occurred in the wave amplitude at the fundamental frequency, due mainly to frictional losses from the partially-standing wavefield which led to a substantial lower transmission coefficient than this. These frictional losses are quantified in Section 4.1. Secondly, there was a striking variation in the amplitude of the first harmonic associated with a beating, in-and-out of phase, of the first Stokes

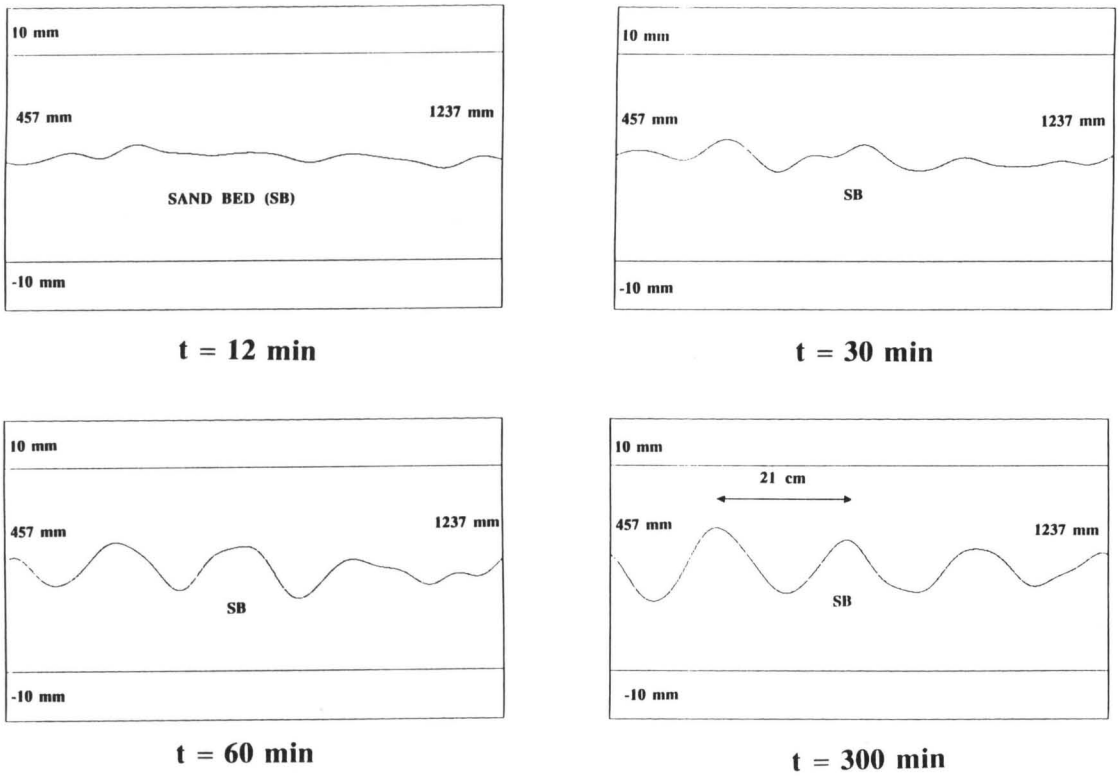

Figure 8. Sequence of bar profiles at different times during the experiment, calculated by an inverse FFT of the appropriate part of the spectrum. The Bragg wavelength (21 cm) is indicated by the arrowed line.

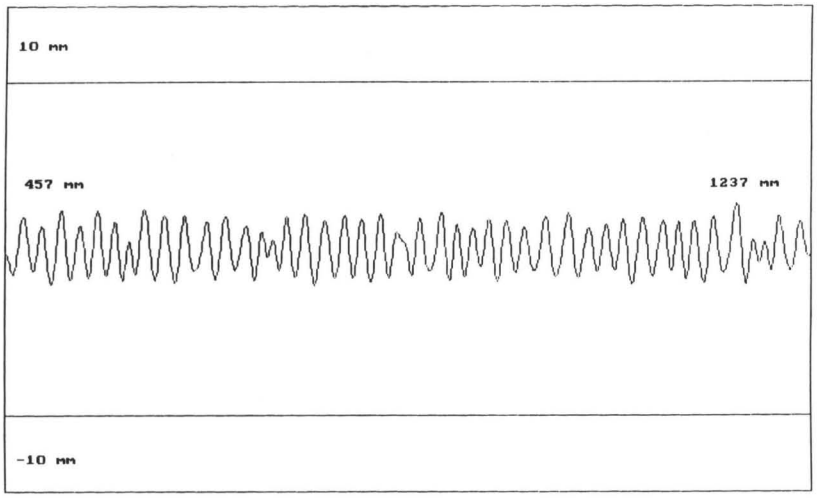

Figure 9. Profile of the ripples after 30 min of wave action, calculated by an inverse FFT of the appropriate part of the spectrum.

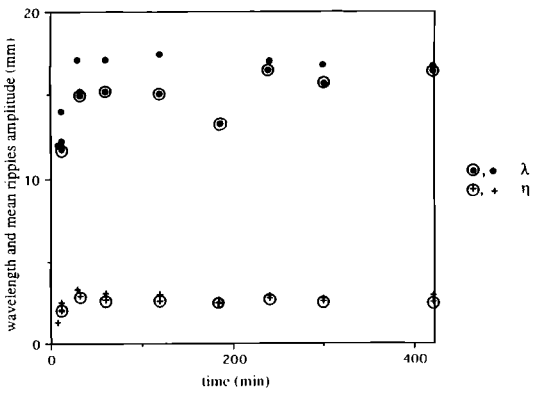

Figure 10. Mean wavelength (λ) and height (η) of ripples through the experiment for a typical sequence of bed profiles (corresponding to Figures 2 to 6). Data corresponding to a second run are labelled with circled symbols.

harmonic (locked on to the fundamental) and an unwanted free wave (generated by the paddle) having twice the fundamental frequency. When the phase velocities of waves with frequencies of 1.5 and 3 Hz in water of depth 6 cm are considered, with phase matching assumed to occur at abscissa x = 0, further matching may be shown to occur at positions having regular spacings of about 62 cm along the tank. This is close to the spacing of 58 cm observed experimentally between successive maxima in the amplitude of the first harmonic. Despite these spatial variations in the first harmonic, it should be noted that the wavefield remained essentially linear throughout the experiment, the percentage of total energy at the fundamental frequency never falling below about 80%.

DISCUSSION

Wave Energy Dissipation

In view of the relatively small reflection coefficients in Table 1 (where R = 0.2 implies reflection of only 4% of the wave energy), it was thought reasonable to make some estimates of the attenuation rate and energy dissipation factor for the (dominant) incident waves alone. Thus the reflected waves were removed from the data in Figures 11a–d by a simple averaging over the partially-standing wave envelope, and an approximate analysis was performed for the incident waves. For both the 'flat bed' and 'sand bed' regions, it was assumed that the incident wave height varied linearly, leading to the results quoted in Table 2 for the nominal wave amplitudes A_w = 4.6 mm and 7.7 mm respectively. As noted earlier, the smaller waves (A_w = 4.6 mm) did not entrain any

Table 2. *Wave characteristics and energy dissipation.*

	Nominal Wave Amplitude A_w = 4.6 mm				Nominal Wave Amplitude A_w = 7.7 mm			
	Flat Bed		Sand Bed		Flat Bed		Sand Bed	
	t = 0	t = 180 min	t = 0	t = 180 min	t = 0	t = 180 min	t = 0	t = 180 min
Representative wave height H (cm)	0.94	0.88	0.90	0.81	1.57	1.51	1.42	1.39
Near bed velocity amplitude U_0 (cm/sec)	4.90	4.59	5.51	4.97	8.19	7.88	8.69	8.55
% Loss of wave height per wavelength	2.4	3.1	2.8	6.0	2.1	3.5	4.4	4.3
Attenuation rate $-\frac{dH}{dx}$	4.81E−4	5.80E−4	5.94E−4	1.153E−3	7.07E−4	1.137E−3	1.477E−3	1.431E−3
$R' = U_0/(2\pi fv)^{1/2}$	15.9	15.0	17.9	16.2	26.7	25.7	28.3	27.9
$f_{e,lam}$ [Laminar flow, smooth bed]	0.104	0.111	0.093	0.103	0.062	0.065	0.059	0.060
f_e [Uncorrected]	0.258	0.354	0.202	0.482	0.136	0.236	0.202	0.202
$f_{e,corr}$ [Corrected for sidewalls]	0.218	0.311	0.175	0.452	0.112	0.211	0.185	0.184
Energy dissipation rate (dyn/cm sec)	5.43	6.39	6.20	11.74	13.01	21.87	25.68	24.46
$\frac{2}{3\pi}\rho f_{e,corr} U_0^3$	5.43	6.39	6.20	11.74	13.01	21.87	25.68	24.46

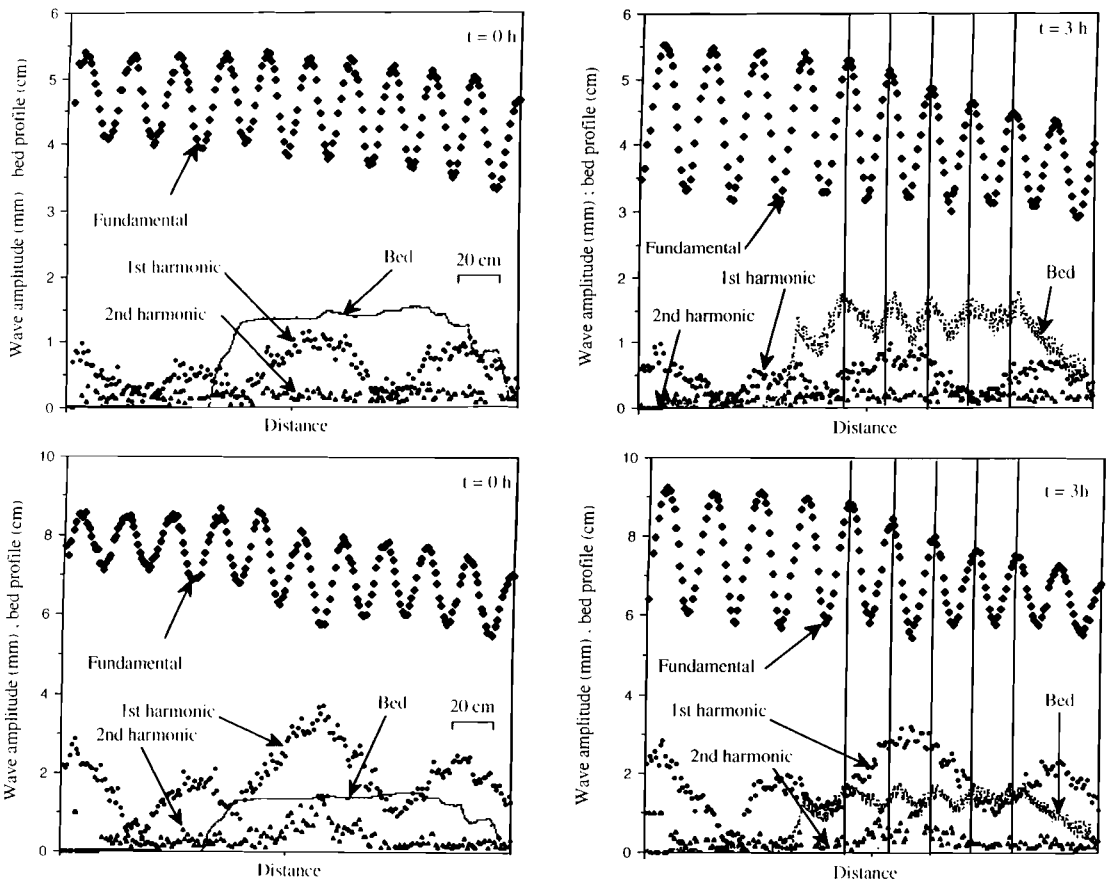

Figure 11. Envelopes for the fundamental and the first two harmonics of the surface wave, and the associated bed profile for different times and incident wave amplitudes A_w: a) Time 0 min, A_w = 4.6 mm. b) Time 0 min, A_w = 7.7 mm. c) Time 180 min, A_w = 4.6 mm. d) Time 180 min, A_w = 7.7 mm.

sediment into suspension, whereas the larger waves (A_w = 7.7 mm) gave rise to a suspended load due to vortex shedding from the rippled bed. At the start of the experiment (t=0) no ripples were present on the region of sand bed for A_w = 4.6 mm, whereas ripples were present almost immediately for A_w = 7.7 mm. At the later time of t = 180 min, the sand bed was rippled in both cases and bars were also present on the bed. It should be emphasized that the results in Table 2 refer only to the dominant component of the waves at the fundamental frequency.

Representative Wave Heights and Near Bed Velocity Amplitudes

The tabulated values H were obtained by averaging the incident wave height over the flat bed and also, separately, over the sand bed region. The mean wave height over the sand was always smaller than that over the flat bed. Moreover, there was a decrease in H from t = 0 to t = 180 min for each of the nominal values of A_w, the probable reason for which is stated below.

The representative wave heights were used to calculate the values of near-bed velocity amplitude (U_0) in Table 2 using linear theory. Like the values of wave height, the velocities above both the flat and sand beds were larger for t = 0 than for t = 180 min for both values of A_w. However, because of the effect of the reduction in water depth over the sand region, the velocities were consistently larger over the sand bed than over the flat bed, for each value of A_w at t = 0 and at t = 180 min.

Wave Height Losses and the Attenuation Rate

The percentage loss of wave height per wavelength and, therefore, the attenuation rate ($-dH/dx$) were less over the flat bed than over the sand bed for each nominal wave height at $t = 0$ and at $t = 180$ min. The rather small percentage loss over the sand bed for the small wave amplitude $A_w = 4.6$ mm at $t = 0$ is explained by the absence of ripples at the start of the experiment. The increase in percentage loss over the flat bed, for both $A_w = 4.6$ mm and 7.7 mm from $t = 0$ to $t = 180$ min, is probably explained by the migration of sand onto the flat bed during the experiment, resulting in the formation of some small ripple feature in this region. It should be noted here that the part of the decrease in the incident wave amplitude due to the development of a reflected wave over the sand region can be neglected in regard of the overall decrease. With a reflection coefficient difference of order 0.12–0.13, the incident wave amplitude is reduced only by 1% at the end of the sand bed. This 'natural' percentage loss of wave amplitude per wave length of about 0.25% is at least 10 times smaller than the overall loss.

Wave Energy Dissipation Factor (f_e) and Dissipation Rate

Following SLEATH (1982), we define the dissipation factor as follows:

$$f_e = (3\pi/2\rho_f U_0^3) \times \{\text{Energy dissipation per unit area of bed per second}\}$$

For a smooth bed and laminar oscillatory flow, it may be shown analytically that

$$f_{e,Lam} = 3\pi\sqrt{2}/8R'$$

where

$$R' = U_0/(2\pi f\nu)^{1/2}$$

where f is the frequency in Hz, and ν the kinematic viscosity. The small size of the tabulated values of R′ indicates that laminar conditions would exist in the boundary layer in each case above a smooth, flat bed, the associated values of $f_{e,Lam}$ being approximately 0.10 for $A_w = 4.6$ mm, and 0.06 for $A_w = 7.7$ mm.

The experimentally derived values are, of course, expected to be larger than these notional laminar values, not least when the bed is rippled and energy dissipation results from vortex shedding. Uncorrected experimental values of f_e have been calculated using the procedure of SLEATH (1982) and, in particular, Sleath's equation (23) which may be written

$$f_e = -(3\pi/4)\cdot dH/dx\cdot\{\text{Sinh}(kh)/(kh)^2\}\cdot\{\text{Sinh}(2kh) + 2kh\}$$

Over the flat bed where the depth $h = 6$ cm, the surface wavelength corresponding to frequency $f_0 = 1.5$ Hz is 46.5 cm (wavenumber $k = 0.135$ cm^{-1}) from the dispersion equation. Over the sand bed where the average depth $h = 4.75$ cm, the wavelength is 42.2 cm ($k = 0.149$ cm^{-1}). These values are in close agreement with estimates of wavelength made from the wave envelopes in Figures 11a–d.

The values of f_e are generally larger for $A_w = 4.6$ mm than for $A_w = 7.7$ mm, and all the values of f_e are larger than the corresponding values of $f_{e,Lam}$ (by a factor of 2 or more) as expected. It should be noted that the experimental values include, not only the effects of friction at the bed, but also dissipation at the sidewalls of the tank and at the free surface. Some account has been taken of sidewall friction by correcting the values of f_e using the simple procedure of DAVIES and HEATHERSHAW (1983, Appendix C). Although this correction reduces the values of f_e somewhat, there remains a substantial difference between $f_{e,Lam}$ and $f_{e,Corr}$, even for the flat bed region at the start of the experiment (when little sand was present on the flat glass bed). This discrepancy may be due to the approximate nature of the calculation of attenuation rate ($-dH/dx$), but it may also be due to the neglect of additional dissipation mechanisms, such as dissipation of energy from the interior of the inviscid flow region, which is channeled into the sidewall boundary layer through the meniscus boundary layer (see MEI, 1983, Sect. 8.3).

The energy dissipation rates (per area), calculated on the basis of the corrected values of f_e, are much larger for $A_w = 7.7$ mm than for $A_w = 4.6$ mm. Also as expected, at both $t = 0$ and $t = 180$ min and for both $A_w = 4.6$ mm and $A_w = 7.7$ mm, the dissipation rates are larger over the sand region than over the flat bed. More generally, it may be concluded from the results that the presence or absence of small-scale ripples is the critical factor which determines the magnitude of the wave energy dissipation rate. The presence or absence of sand bars is of only minor importance in this context, as may be judged from the closely similar results for f_e (and energy dissipation rate) for $A_w = 7.7$ mm at both $t = 0$ and $t = 180$ min.

Ripple Formation

The threshold velocity for ripple formation on the initially flattened bed was observed at U_0 = 8.2 cm/sec. This may be compared with values for the threshold of sediment motion on a flat bed given by the formulae of BAGNOLD (1946) and KOMAR and MILLER (1975). Using the present experimental parameters, Bagnold's formula for the "first motion" (*i.e.*, incipient motion) of grains on a flat bed, in what was stated by Bagnold to be a laminar boundary layer flow, yields U_0 = 5.0 cm/sec. KOMAR and MILLER'S formula which is based on the results of several laboratory studies yields U_0 = 5.9 cm/sec.

The mean values of ripple wavelength (λ) and height (η), averaged over the bed profile in Figure 11 after t = 180 min, were of λ = 1.3 cm and η = 2.3 mm respectively, corresponding to a ripple steepness η/λ = 0.18. (As noted earlier, there was a tendency for the largest ripples to occur on the bar crests.) Taking the representative velocity amplitude over the sand region as U_0 = 8.6 cm/sec it follows that the orbital diameter of the near-bed fluid particles was about $d_0 = U_0/\pi f_0$ = 1.83 cm. Hence the ratio λ/d_0 was 0.71 which is quite close to the value of 0.65 found by MILLER and KOMAR (1980) and of ⅔ found by LOFQUIST (1978) during the early stages of ripple formation in each case. The present results have also been compared with the values of λ and η given by the formulae of NIELSEN (1979) which are based on a variety of laboratory data sets. For the present representative value of the mobility number M = 5.54 ($M = U_0^2/\gamma gD$) and friction factor f′ = 0.0304 (relating to skin friction only), Nielsen's formulae yield η = 2.0 mm, λ = 1.16 cm (η/λ = 0.18) in good agreement with the experimental values.

Bar Formation

Provided that the near-bed oscillatory flow beneath partially-standing waves gives rise to sediment motion, sand bars may be expected to form having wavelength equal to approximately half the surface wavelength (in accordance with the Bragg condition). As noted earlier, the positioning of the bars' crests in relation to the wave envelope, and hence the ability of the bar system to reflect incident waves, depends upon the dominant sediment transport mechanism (*i.e.*, 'bedload' or 'suspended' load). In the present experiments, the dominant mechanism was near-bed transport associated with vortex shedding from sand ripples and the developing bars (with crests on the down-wave side of the antinodes of elevation) brought about a significant increase in the reflection coefficient through the experiment.

In laboratory experiments of the present kind, there is in practice a rather small 'operating window' between low waves which are of insufficient size to move sediment and steep waves which move sediment very readily but are rather nonlinear and, possibly, unstable. It was observed in the present experiments that, although sand ripples formed very rapidly in the latter case, a regular bar patch did not necessarily develop. Another observation was that, if a run was started just above the threshold of sand motion, the development of ripples and bars was very sensitive to subsequent small variations in the local water depth. The presence of small irregularities on the initially flattened sand surface was also a factor of importance. It may be concluded that the initial conditions must lie in a fairly narrow range if regular, stable bars are to develop.

As noted earlier, the bar spacing in the present experiments was roughly half the surface wavelength and was such that the reflection coefficient on the up-wave side of the sand patch increased during the experiment by 0.12 for A_w = 4.6 mm and by 0.13 for A_w = 7.7 mm (see Table 1). In order to make a general assessment of the reflectivity of the bar patch, wave propagation over the bed profile at time t = 180 min has been examined using the linear, potential model of REY (1992). For this purpose, the bed was treated as fixed and beach-back reflection was assumed to be zero. For waves having frequency in the range 1–2 Hz, the predicted reflection coefficient (R) on the up-wave side of the bar patch is as shown in Figure 12. At the experiment frequency of f_0 = 1.5 Hz, the reflection coefficient is about 0.13, which is in agreement with the increase in R during the experiment for A_w = 7.7 mm (Table 1). More generally, the results show a strongly oscillatory behaviour in R in the frequency range 1 to 2 Hz, with a maximum value of R (= 0.18) predicted at f = 1.4 Hz. This may be attributed both to slight irregularities in the bar spacing (Figure 11c), and also to the 'finite' size of the bars (in relation to the mean water depth). The shift to low frequency of the maximum reflection coefficient, compared with the forcing (Bragg) frequency (of 1.5 Hz), has been discussed by BELZONS *et al.* (1991) for the case of a fixed bed.

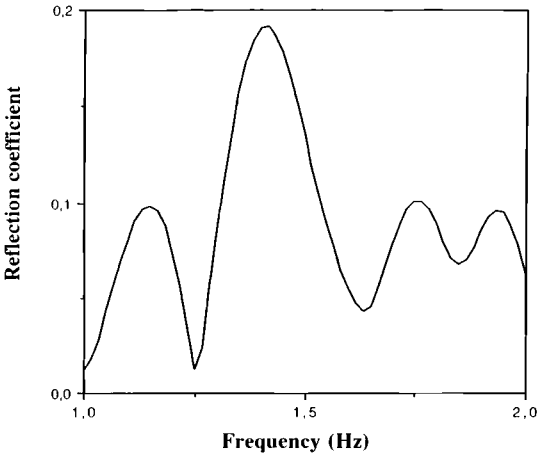

Figure 12. Numerical calculation of the reflection coefficient for the bed profile after 180 min of wave action. The profile is one dimensional and considered as fixed, and the model (REY, 1992) is linear and potential.

CONCLUSION

In previous experimental studies carried out at Marseille, it has been shown that the main features of the interaction between surface waves and regular or irregular, fixed, bed profiles (*i.e.*, reflection coefficient, Bragg resonance, localization, and the effects of vorticity and nonlinearity) can be accurately observed in a small-scale wave tank (BELZONS *et al.*, 1988; BELZONS *et al.*, 1991; GUAZZELLI *et al.*, 1992; REY *et al.*, 1992). In the present study, the capabilities of the experimental set-up have been extended in order to examine in detail the correlated evolution of the profile of an erodible sand bed and a field of partially-standing waves.

A very accurate, rapid ultra-sonic detection system was used to monitor the evolution of an initially flattened sand bed, including both the early formation of small-scale ripples and the longer-term development of a patch of stable sand bars. The associated evolution of the surface waves was also monitored using an ultra-sonic sensor, with which the harmonic composition of the wavefield was determined.

The main findings of the present study were as follows:

(1) Small-scale ripples formed rapidly on the initially flattened bed with wavelengths and heights related to position in the partially-standing wave envelope. The threshold for the ripple formation was found to be slightly above the threshold for sediment motion on a flat bed given by the criteria of BAGNOLD (1946) and KOMAR and MILLER (1975) for the present experimental conditions. Ripple sizes varied as bars formed during the experiment, with larger ripples ultimately becoming established on the bar crests and smaller ripples in the troughs.

(2) Sand bars formed with wavelength equal to approximately half the surface wavelength, thus satisfying the Bragg condition. The bar crests formed slightly down-wave of the antinodes of elevation as a result of a net, near-bed sediment transport due to vortex shedding from the (asymmetrical) ripples. As the bars grew, the up-wave reflection coefficient increased, as expected for this positioning of bars relative to the wave envelope (O'HARE and DAVIES, 1990).

(3) A linear, potential model (REY, 1992) was used to predict the reflection coefficient of the region of sand bars after 180 min of wave action. (The bed was considered here to be fixed, and the wave frequency was varied through the range 1 to 2 Hz.) The predicted reflection coefficient of 0.13 at the operating experimental frequency of 1.5 Hz was in good agreement with the increase in the reflection coefficient during the experiment (in which there was a small initial amount of beach-back reflection). More generally, the reflection coefficient was highly oscillatory in the range of frequencies investigated, having a maximum value of 0.18 at frequency 1.4 Hz. This shift of maximum reflection to a lower frequency than the forcing frequency is expected for fixed bars of 'finite' amplitude in shallow water (BELZONS *et al.*, 1991).

(4) The reflection coefficient was not influenced significantly by bottom friction and sediment movement, the flow being effectively inviscid away from the boundaries of motion. Wave energy dissipation was due largely to vortex shedding from the small-scale ripples but was complicated by frictional losses at the sidewalls of the tank and also at the free surface. Measurements of wave height attenuation made from the wave envelope suggested that the values of wave dissipation factor (f_c) for the rippled beds were 3 or 4 times larger than the equivalent values for laminar flow over a smooth surface.

Further experimental work is in progress at Marseille to determine more precisely the initial

conditions required for the formation of a stable bar system, as well as the evolution of that system under the action of detuned surface waves.

ACKNOWLEDGEMENTS

The experimental work presented here formed part of the doctoral thesis of V. Rey, in which further information may be found. We gratefully acknowledge the contribution of Roland Faure, Engineer at the IUSTI, who designed and constructed the ultrasonic detection systems for both the bed and surface wave profiles. One of us (A.G.D.) benefitted from a one month visit to Marseille in 1991, as associated Professor of the Université de Provence, during which this work was initiated.

LITERATURE CITED

BAGNOLD, R.A., 1946. Motion of waves in shallow water. Interaction between waves and sand bottoms. *Proceedings of the Royal Society of London, Series A,* 187, 1–8.

BELZONS, M.; GUAZZELLI, E., and PARODI, O., 1988. Gravity waves on a rough bottom: Experimental evidence of one-dimensional localization. *Journal of Fluid Mechanics,* 186, 539–558.

BELZONS, M.; REY, V., and GUAZZELLI, E., 1991. Subharmonic Bragg resonance for surface water waves. *Europhysics* Letters, 16(2), 189–194.

BOWEN, A.J., 1980. Simple models of nearshore sedimentation; beach profiles and longshore bars. *In:* MCCAHN, S.B. (ed.), The Coastline of Canada. *Geological Survey, Paper 80-10,* 1–11.

BROOKE-BENJAMIN, T.; BOCZAR-KARAKIEWICZ, B., and PRITCHARD, W.G., 1987. Reflection of water waves in a channel with corrugated bed. *Journal of Fluid Mechanics,* 185, 249–274.

CARTER, T.G.; LIU, P.L.-F., and MEI, C.C., 1972. Mass transport by waves and offshore sand bedforms. *Proceedings (ASCE),* 99, Journal of Waterways, Harbors and Coastal Engineering Division, WW2, 165–184.

DAVIES, A.G., 1982. The reflection of wave energy by undulations of the seabed. *Dynamics of Atmospheres and Oceans,* 6, 207–232.

DAVIES, A.G. and HEATHERSHAW, A.D., 1983. Surface-wave propagation over sinusoidally varying topography: Theory and observation. *Institute of Oceanographic Sciences, Report No. 159,* 181p. (in 2 parts).

DAVIES, A.G. and HEATHERSHAW, A.D., 1984. Surface-wave propagation over sinusoidally varying topography. *Journal of Fluid Mechanics,* 144, 419–443.

DETTE, H.H., 1980. Migration of longshore bars. *Proceedings of the 17th International Conference on Coastal Engineering,* (ASCE), 1476–1492.

GUAZZELLI, E., REY, V., and BELZONS, M., 1992. Higher-order Bragg reflection of gravity surface waves by periodic beds. *Journal of Fluid Mechanics,* in press.

HEATHERSHAW, A.D. and DAVIES, A.G., 1985. Resonant wave reflection by transverse bed forms and its relation to beaches and offshore bars. *Marine Geology,* 62, 321–338.

JOHNS, B., 1970. On the mass transport induced by oscillatory flow in a turbulent boundary layer. *Journal of Fluid Mechanics,* 43, 177–185.

KOMAR, P.D. and MILLER, M.C., 1975. Sediment threshold under oscillatory waves. *Proceedings of the 14th International Conference on Coastal Engineering, 1974,* (ASCE), pp. 756–775.

LOFQUIST, K.E.B., 1978. Sand ripple growth in an oscillary flow water tunnel. *Technical Paper No. 78-5,* US Army Corps of Engineers, Coastal Engineering Research Center, 101p.

LONGUET-HIGGINS, M.S., 1953. Mass transport in water waves. *Philosopical Transactions of the Royal Society of London,* Series A, 245, 535–581.

MEI, C.C., 1983. *The Applied Dynamics of Ocean Surface Waves.* New York: Wiley, 740p.

MILLER, M.C. and KOMAR, P.D., 1980. Oscillation sand ripples generated by laboratory apparatus. *Journal of Sedimentary Petrology,* 50, 1, 173–182.

NIELSEN, P., 1979. Some basic concepts of wave sediment transport. Technical University of Denmark, *Institute of Hydrodynamics and Hydraulic Engineering, Series Paper No. 20,* 160p.

O'HARE, T. and DAVIES, A.G., 1990. A laboratory study of sand bar evolution. *Journal of Coastal Research,* 6(3), 531–544.

O'HARE, T.J., 1992. Sand bar evolution beneath partially-standing waves: Laboratory experiments and model simulations. Ph.D. dissertation, University of Wales, 206p.

REY, V., 1991. Propagation d'ondes de gravité au dessus de fonds solides ou constitués de sédiments: application à l'étude d'interactions ondes-sédiments. Thèse, Université de Provence.

REY, V., 1992. Propagation and local behaviour of normally incident gravity waves over varying topography. *European Journal of Mechanics.* B (Fluids), 11(2), 213–232.

REY, V.; BELZONS, M., and GUAZZELLI, E., 1992. Propagation of surface gravity waves over a rectangular submerged bar. *Journal of Fluid Mechanics,* 235, 453–479.

SAYLOR, J.H., and HANDS, E.B., 1970. Properties of longshore bars in the Great Lakes. *Proceedings of the 12th International Conference on Coastal Engineering, 1970,* (ASCE), pp. 839–853.

SCOTT, T., 1954. Sand movement by waves. *Technical Memorandum, Number 48,* U.S. Army Corps of Engineers, Beach Erosion Board, 37p.

SHORT, A.D., 1975a. Offshore bars along the Alaskan Arctic coast. *Journal of Geology,* 83, 209–221.

SHORT, A.D., 1975b. Multiple offshore bars and standing waves. *Journal of Geophysical Research,* 80, 3838–3840.

SLEATH, J.F.A., 1982. Friction coefficients of rippled beds in oscillatory flow. *Continental Shelf Research,* 1, 1, 33–47.

□ RÉSUMÉ □

Des barres de sable ayant un espacement égal à la demi longueur d'onde de l'onde de surface peuvent être formées par l'action d'ondes partiellement stationnaires sur un fond érodible. On a étudié ici les étapes de la formation d'un ensemble de barres dans un canal à houle, en utilisant des systèmes de détection à ultrasons pour suivre à la fois l'évolution du profil du fond et celle de l'onde de surface. Initialement des rides de faible taille se forment sur la surface (aplanie) du fond. Ces rides ont une taille variable en fonction de leur position par rapport à l'enveloppe de l'onde et ont un profil assymétrique dû à l'assymétrie du mouvement oscillant prés du fond. L'émission de vortex à partir de ces rides produit une accumulation (crêtes des barres) et une érosion (creux) en relation avec la position par rapport à l'enveloppe de l'onde. Les barres se forment avec une longueur d'onde satisfaisant à la condition de Bragg et les crêtes situées en aval des ventres de l'onde de surface. Comme on doit s'y attendre, ceci conduit à une augmentation du coefficient de réflection global de l'ensemble des barres au cours de leur croissance. La présence de rides de faible taille n'a qu'un effet mineur sur le coefficient de réflection car l'écoulement est essentiellement inviscide loin des parois, et la longueur d'onde des rides est bien plus faible que celle de l'onde de surface. Cependant ces rides jouent un rôle important pour la dissipation de l'énergie dans le canal, les facteurs de dissipation de londe étant 3 à 4 fois plus grands que leurs homologues pour un écoulement laminaire au-dessus d'un fond lisse. On peut penser que les observations de l'interaction résonante entre onde de surface et fond érodible décrites ici, sont les plus détaillées et précises à avoir été présentées à cette date.